Improved image deblurring with anti-reflective boundary conditions and re-blurring

(This is a preprint of an article published in Inverse Problems, 22 (2006) pp. 2035-2053.)

M. Donatelli†, C. Estatico‡, A. Martinelli†, and S. Serra-Capizzano†

†Dipartimento di Fisica e Matematica, Università dell'Insubria - Sede di Como, Via Valleggio 11, 22100 Como, Italy
‡Dipartimento di Matematica, Università di Genova, Via Dodecaneso 35, 16146 Genova, Italy

E-mail: marco.donatelli@uninsubria.it, estatico@dima.unige.it, andrea.martinelli@uninsubria.it, stefano.serrac@uninsubria.it

Abstract. Anti-reflective boundary conditions (BCs) have been introduced recently in connection with fast deblurring algorithms. In the noise free case, it has been shown that they reduce substantially artifacts called ringing effects with respect to other classical choices (zero Dirichlet, periodic, reflective BCs) and lead to $O(n^2 \log(n))$ arithmetic operations, where n^2 is the size of the image. In the one-dimensional case, for noisy data, we proposed a successful approach called re-blurring: more specifically, when the PSF is symmetric, the normal equations product $A^T A$ is replaced by A^2, where A is the blurring operator (see Donatelli et al. Inverse Problems, 21, pp. 169–182). Our present goal is to extend the re-blurring idea to nonsymmetric PSFs in 2 dimensions. In this more general framework, suitable for real applications, the new proposal is to replace A^T by A' in the normal equations, where A' is the blurring matrix related to the current BCs with PSF rotated by 180 degrees. We notice that, although with zero Dirichlet and periodic BCs the re-blurring approach is equivalent to the normal equations scheme, since there $A' = A^T$, the novelty concerns both reflective BCs and anti-reflective BCs, where in general $A' \neq A^T$. We show that the re-blurring with anti-reflective BCs is computationally convenient and leads to a large reduction of the ringing effects arising in classical deblurring schemes. A wide set of numerical experiments concerning 2D images and nonsymmetric PSFs confirms the effectiveness of our proposal.

AMS classification scheme numbers: 65F10, 65F15, 65Y20

Submitted to: *Inverse Problems*

1. Introduction

We consider the classical deblurring problem of blurred and noisy images with space invariant PSFs. More precisely, after standard discretization of a Fredholm equation of first kind with

shift-invariant kernel (see e.g [3]), the discrete mathematical model of image blurring and noising is described by a system whose i-th equation is as follows

$$g_i = \sum_{j\in\mathbb{Z}^2} f_j h_{i-j} + \nu_i\,, \qquad i \in \mathbb{Z}^2. \tag{1}$$

Here, for $s \in \mathbb{Z}^2$, the mask $h = (h_s)$ represents the (discrete) blurring operator (the discrete PSF), $\nu = (\nu_s)$ is the noise contribution, $g = (g_s)$ is the blurred and noisy observed object, and $f = (f_s)$ represents an approximation of the true object. In analogy with the continuous setting, given h and some statistical knowledge of ν, the problem is to recover the unknown "true" image $f = (f_s)$ in a fixed field of view (FOV) described by $s \in \{1,\dots,n\}^2$ from the knowledge of $g = (g_s)$ in the same window only. It is clear that the system described by (1) with i ranging in $\{1,\dots,n\}^2$ is under-determined, that is, the number of unknowns exceeds the number of equations, since we have n^2 equations and $(n+q-1)^2$ unknowns involved, when the support of the discretized PSF is a square of size $q^2 > 1$. In order to take care of this problem we can follow different approaches: for instance in [8] the authors proposed a statistical approach based on the reconstruction of the image on a domain broader than the FOV, in [5] it was shown how to work with the rectangular matrix arising from (1) in the case of the Richardson-Lucy method and the same approach was applied to least-squares problems in [24], finally in several papers appropriate choices of the so-called boundary conditions (BCs) are employed (see e.g. [9, 23]). The latter strategy consists in the reduction of the system (1) in a square system of size n^2, where the unknowns outside the FOV are defined as affine relations between the unknowns inside the FOV. However, if the considered BCs are unphysical and even when the noise is not present, then special artifacts, related to the Gibbs phenomenon and called ringing effects, appear in the reconstruction especially close to the boundary. We count zero Dirichlet, periodic, reflective (also called Neumann or symmetric), and anti-reflective (see [3, 19, 23] and references therein). In the noise free case, it has been shown that the anti-reflective BCs (AR-BCs) are the most precise [23], in the sense that no discontinuity in the image or in its normal derivative is artificially added by the imposed BCs. Therefore, the ringing effects are negligible with respect to the other BCs (see [23, 10]). Moreover, from a computational point of view, the AR-BCs show essentially the same favorable behavior as the reflective BCs (R-BCs). Indeed, the associated structure seems a bit involved, since it is block Toeplitz + Hankel with Toeplitz + Hankel blocks plus a structured low rank matrix. Despite the apparent complicate expression of the resulting matrix, the product is again possible by two-level fast Fourier transforms (FFTs), see Subsection 3.5 for details, while the solution of a linear system can be obtained in $O(n^2\log(n))$ real operations by uni-level and two-level fast sine transforms (FSTs), if the PSF is strongly symmetric [23, 10]. We write that a PSF h is strongly symmetric if it is symmetric with respect to each direction: formally $h_{i,j} = h_{|i|,|j|}$, $\forall\, i,j \in \mathbb{Z}$ (see e.g. [16]). In [24] the approach firstly proposed in [5] for the Richardson-Lucy method was applied to least-squares image deconvolution problems and compared with the BCs approach in terms of the quality of the restored images. In real applications the quality of the restored images is slightly better than that with AR-BCs. However the main limit of such strategy is that it can be applied only with iterative methods and we cannot solve e.g. the Tikhonov linear system using few fast trigonometric transforms. On the other hand, in the case of strongly symmetric PFSs, this can be done with the AR-BCs and the re-blurring strategy as we will show in this paper. In addition, if the PSF is strongly symmetric the matrix vector product with AR-BCs and after pre-processing requires essentially two d-dimensional FSTs of size n^d, while the approach in [24] requires two d-dimensional FFTs of size $(2n)^d$. In terms of algebraic operations applying a fast trigonometric transform of size

$(2n)^d$ instead of n^d increases the cost by a factor close to 2^d. Since A^2 is still an AR-BCs matrix if A is, it is clear that a matrix vector product with A^2 costs again two FSTs, while the technique in [24], involving at each iteration a matrix vector product with the rectangular matrices A and A^T, costs after pre-processing four FFTs of size $(2n)^d$. Moreover for the FFT it is necessary to use complex arithmetics, while the FST uses only real operations and this is more than a factor two (e.g. it is a factor three considering only multiplication operations). By summarizing, in the case of strongly symmetric PFSs, with the approach in [24] one iteration of an iterative regularization method is more expensive than 2^{d+2} iterations with AR-BCs and often the restored image is only slightly better or comparable. On the other side, regarding the approach discussed in [8] the comparison with the use of appropriate BCs is more difficult, since the only numerics discussed in that paper concern Dirichlet BCs: however, while there is a slight improvement with respect to these less precise BCs in terms of image quality, it seems that there is no improvement concerning the computational cost and a comparison with the more precise reflective and anti-reflective BCs is not present.

Furthermore, it is worth noticing that recently the AR-BCs have been extended to a d dimensional setting with arbitrary $d \geq 1$. The resulting algebra of matrices called AR-algebra has been studied and $O(n^d \log(n))$ real procedures for the solution of a linear system of size n^d have been described again in the case of strong symmetry, i.e., $h_s = h_{|s|}$, $\forall\, s \in \mathbb{Z}^d$, with $s = (s_1, \ldots, s_d)$ and $|s| = (|s_1|, \ldots, |s_d|)$ (see [2]). In the case of noisy signals, the application of standard regularizing procedures, which are necessary for handling the effect of the noise, was considered. Regarding the AR-BCs, the negative surprise was a partial loss of the favorable computational features and, in some cases, a deterioration of the reconstruction quality with a moderate level of noise: indeed, dealing with the AR-BCs in some one-dimensional examples, the restoration quality may deteriorate when the signal-to-noise ratio (SNR) decreases. Therefore, in [12, 11], we modified the classical regularization techniques in order to exploit the quality of the AR-BCs reconstruction and the efficiency of the related numerical procedures: we called this idea re-blurring. In this paper we consider nonsymmetric PSFs with special attention to the two-dimensional (2D) case of classical images. Indeed, when dealing with noisy objects, we have several choices: the use of iterative regularization [13] for normal equations such as Landweber, conjugate gradient for normal equations (CGNE) etc., or the application of a Tikhonov regularization procedure [3] with direct or iterative solution of the associated parametric system. A common point is the use the normal equation and therefore of $A^T A$ where A is the matrix obtained with one of the chosen BCs.

In this paper, in the more difficult case of 2D problems and nonsymmetric PSFs, we will show that a more general re-blurring scheme is to replace A^T by A' in all the above algorithms, where A' is the matrix associated with the original PSF rotated by 180 degrees: in the specific case of signals with symmetric PSFs, it is worth noting that A' and A are the same matrix and therefore the new proposal reduces to the one in [12]. By using an embedding trick, we prove that the new formulation with $A'A$ for the AR-BCs overcomes the computational difficulties due to a low rank term in the product $A^T A$, refer to Subsection 3.5. Under the assumption of strong symmetry of the PSF and under mild support conditions, the restored image with n^2 pixels can be computed in $O(n^2 \log(n))$ real operations by using few two-level FSTs and the re-blurred Tikhonov-like equations

$$\left[A'A + \mu \mathcal{T}'\mathcal{T}\right] \mathbf{f} = A'\mathbf{g}, \tag{2}$$

where $\mathcal{T}$ is any even discrete differential operator with the AR-BCs. In the d-dimensional case, as shown in [2], the operation $A \mapsto A'$ can be defined in a natural way. Moreover, according to the analysis in [2], the cost of solving the re-blurred system (2) is still $O(n^d \log(n))$ where

n^d is the size of the restored object, provided that the PSF is again strongly symmetric i.e. $h_s = h_{|s|}$, $\forall\, s \in \mathbb{Z}^d$. By a theoretical point of view, it is important to remark that such strong symmetry of the PSF is fulfilled in several models in real optical applications. For instance, in most 2D astronomical imaging with optical lens [3], the model of the PSF is circularly symmetric, and hence, strongly symmetric; in the multi-image de-convolution of some recent interferometric telescopes, the PSF is strongly symmetric too (see Figure 1 of [4]). On the other hand, it is important to remark that in real applications some optical distortions may be present, which cause asymmetries in the PSF. Although most of these distortions may be identified and corrected by interchanging special optical lens, the experimental PSF may come out nonsymmetric anyway. Moreover, in real applications when the PSF is obtained by measurements (like a guide star in astronomy), the influence of noise lead to a numerically nonsymmetric PSF, also when the kernel of the PSF is strongly (or centro) symmetric. In such a case, by employing a symmetrized version of the measured PSF, we observe comparable (sometimes also better) restorations (see [15, 1]).

In any case, it is worth stressing that the application of our new re-blurring approach with AR-BCs is robust with respect to asymmetries: indeed, we always observed quite good results, not only in these real settings of weak asymmetry, but also in the case of general PSFs with arbitrary levels of asymmetry (see Section 4).

The paper is organized as follows: in Section 2 we briefly review the algebraic properties of the linear systems arising from d-dimensional AR-BCs with special attention to the case where $d = 1, 2$. In Section 3 we discuss the re-blurring idea by a theoretical and a computational point of view, and in Section 4 we report and discuss several 2D numerical experiments that confirm the effectiveness of the proposal, by including nonsymmetric examples as well. Section 5 is devoted to conclusions and to a discussion on future directions of research.

2. Linear systems with AR-BCs

This section is devoted to illustrate the algebraic and computational features of some noteworthy classes of matrices and to show that the AR-BCs approach leads to matrices related or belonging to such classes. More specifically, in Subsection 2.1 we first introduce the d-level τ class related to the d-level discrete sine transforms, $d \geq 1$, and then we briefly describe the d-dimensional AR-algebras. Finally, in Subsection 2.2 we give a concise description of the AR-BCs in the case of signals and images ($d = 1, 2$).

2.1. The τ and AR-algebras

Let Q be the type I sine transform matrix of order n (see [6]) with entries

$$[Q]_{i,j} = \sqrt{\frac{2}{n+1}} \sin\left(\frac{ji\pi}{n+1}\right), \quad i, j = 1, \ldots, n. \tag{3}$$

It is known that the real matrix Q is orthogonal and symmetric ($Q = Q^T$ and $Q^2 = I$). For any n dimensional real vector $\mathbf{v}$, the matrix vector multiplication $Q\mathbf{v}$ can be computed in $O(n \log(n))$ real operations by using the algorithm DST I. In the multidimensional case, setting $Q^{(d)} = Q \otimes \cdots \otimes Q$ (d times, $\otimes$ being the Kronecker product, see [14]) and by considering $\mathbf{v} \in \mathbb{R}^{n^d}$, the vector $Q^{(d)}\mathbf{v}$ can be computed in $O(n^d \log(n))$ real operations by the DST I procedure of level d. For every integer $d \geq 1$ we define $\tau^{(d)}$ as the space of all the d-level matrices that can be simultaneously diagonalized by $Q^{(d)}$. Formally we have

$$\tau^{(d)} = \{Q^{(d)} D Q^{(d)} : \ D \text{ is a real diagonal matrix of size } n^d\}. \tag{4}$$

Accordingly, for $d \geq 1$ integer number, we define the classes of d-level $n^d \times n^d$ matrices $\mathcal{S}_d$ as follows. For $d = 1$, $M \in \mathcal{S}_1$ if

$$M = \begin{bmatrix} \alpha & & \\ \mathbf{v} & \hat{M} & \mathbf{w} \\ & & \beta \end{bmatrix}, \tag{5}$$

with $\alpha, \beta \in \mathbb{R}$, $\mathbf{v}, \mathbf{w} \in \mathbb{R}^{n-2}$, and $\hat{M} \in \tau^{(1)}_{n-2}$. For $d > 1$, in short, the external structure is block $\mathcal{S}_1$ with blocks belonging to $\mathcal{S}_{d-1}$. More precisely, $M \in \mathcal{S}_d$ if

$$M = \begin{bmatrix} \alpha & & \\ \mathbf{v} & M^* & \mathbf{w} \\ & & \beta \end{bmatrix}, \tag{6}$$

with $\alpha, \beta \in \mathcal{S}_{d-1}$, $\mathbf{v}, \mathbf{w} \in \mathbb{R}^{(n-2)n^{d-1} \times n^{d-1}}$, $\mathbf{v} = (v_j)_{j=1}^{n-2}$, $\mathbf{w} = (w_j)_{j=1}^{n-2}$, $v_j, w_j \in \mathcal{S}_{d-1}$ and $M^* = \left(M^*_{i,j}\right)_{i,j=1}^{n-2}$ having external $\tau^{(1)}_{n-2}$ structure such that every block $M^*_{i,j}$ of M^* belongs to $\mathcal{S}_{d-1}$. Notice that in the previous block matrices the presence of blanks indicates zeros or block of zeros of appropriate dimensions.

In [2], for every fixed d, it is shown that the class $\mathcal{S}_d$ is an algebra of matrices i.e. $\mathcal{S}_d$ is closed under linear combinations, multiplication, and therefore inversion. Moreover it allows fast computations as the next Theorem 2.1 shows.

Theorem 2.1 [2] *Let $\mathbf{f} = [\mathbf{f}_j]_{j=1}^n$ and $\mathbf{g} = [\mathbf{g}_j]_{j=1}^n$ be two vectors with real entries and size n^d, being each $\mathbf{f}_j$, $\mathbf{g}_j$ a vector of n^{d-1} components. Under the notations in (5) and (6), the following statements are true:*

(i) every linear system $M\mathbf{f} = \mathbf{g}$ with $M \in \mathcal{S}_d$ can be solved in $O(n^d \log(n))$ arithmetic (real) operations, whenever M is an invertible matrix;

(ii) every matrix vector product $\mathbf{g} := M\mathbf{f}$ with matrix $M \in \mathcal{S}_d$ costs $O(n^d \log(n))$ arithmetic (real) operations;

(iii) the eigenvalues of M are given by those of α, those of β, and those of M^* ($M^* = \hat{M}$ if $d = 1$), and their computation can be obtained within $O(n^d \log(n))$ arithmetic (real) operations;

(iv) the space $\mathcal{S}^{(d)}$ is an algebra, i.e., it is closed under linear combinations, product and inversion and its dimension, as vector space, is $(3n-4)^d$.

The $O(n^d \log(n))$ recursive algorithm proposed in the proof of point *(i)* of Theorem 2.1 in [2] can be used for solving any linear system where the coefficient matrix belongs to the $\mathcal{S}_d$ class. In particular, this is the case when A is an AR-BCs matrix with strongly symmetric PSF, satisfying a proper support condition, and the coefficient matrix is $A'A + \mu\mathcal{T}'\mathcal{T}$ where $\mathcal{T}$ is any even differential operator with AR-BCs, i.e., when the re-blurring strategy is used: in that case $A' = A \in \mathcal{S}_d$, $\mathcal{T}' = \mathcal{T} \in \mathcal{S}_d$, and therefore $A'A + \mu\mathcal{T}'\mathcal{T} \in \mathcal{S}_d$ due to structure of algebra of $\mathcal{S}_d$. A sketch of an explicit non recursive algorithm for the 2D case is described in [10] for matrices arising from AR-BCs; the general case is reported in [2].

2.2. AR-BCs and the AR-algebra

We have already mentioned that, in the generic case, periodic and zero Dirichlet BCs introduce a discontinuity in the signal, while the R-BCs preserve the continuity of the signal, but introduce a discontinuity in the derivative (the normal derivative when $d = 2$). Our approach is to use an anti-reflection: in this way, at the boundaries, instead of having a mirror-like symmetry around the vertical axis (R-BCs), we impose a global symmetry around the boundary points: for $d = 1$ the latter choice corresponds to a central symmetry around the considered boundary point, while for $d = 2$ we have a symmetry around the straight line supporting the considered segment of the boundaries. More specifically, in the one-dimensional case, if f_1 is the left boundary point and the f_n is the right one, then the external points f_{1-j} and f_{n+j}, $j \geq 1$, are computed as function of the internal points according to the rules $f_{1-j} - f_1 = -(f_{j+1} - f_1)$ and $f_{n+j} - f_n = -(f_{n-j} - f_n)$. If the support of the centered blurring function is $q = 2m + 1 \leq n$, then we have

$$\begin{aligned} f_{1-j} &= f_1 - (f_{j+1} - f_1) = 2f_1 - f_{j+1}, \qquad \text{for all } j = 1, \ldots, m, \\ f_{n+j} &= f_n - (f_{n-j} - f_n) = 2f_n - f_{n-j}, \qquad \text{for all } j = 1, \ldots, m. \end{aligned}$$

If the blurring function (the PSF) h is symmetric (i.e., $h_j = h_{-j}, \forall\, j \in \mathbb{Z}$), if $h_j = 0$ for $|j| > n - 3$ (support/degree condition), and h is normalized as $\sum_{j=-m}^{m} h_j = 1$, then the structure of the $n \times n$ 1D anti-reflective blurring matrix A is a special case of (5) with $\alpha = \beta = 1$, $v_j = w_{n-1-j} = h_j + 2\sum_{k=j+1}^{m} h_k$, and with $\hat{M}$ being the $\tau_{n-2}^{(1)}$ matrix with j-th eigenvalue given by $h(x) = h_0 + 2\sum_{k=1}^{m} h_k \cos(kx)$ evaluated at $x_j^{(n)} = j\pi/(n-1)$, $j = 1, \ldots, n-2$ (see [23]). Therefore the spectrum of the blurring matrix A is given by 1 with multiplicity 2 and by the eigenvalues of $\hat{M}$.

The AR-BCs naturally extend to two dimensions. In particular, for a blurring operator represented by a $q \times q$ centered PSF with $q = 2m + 1$, the point $f_{1-j,t}$, $1 \leq j \leq m$, $1 \leq t \leq n$, is represented by $2f_{1,t} - f_{j+1,t}$. Analogously, for $1 \leq j \leq m$, $1 \leq s, t \leq n$, we have $f_{s,1-j} = 2f_{s,1} - f_{s,j+1}$, $f_{n+j,t} = 2f_{n,t} - f_{n-j,t}$ and $f_{s,n+j} = 2f_{s,n} - f_{s,n-j}$. It is important to notice that, when both indices lie outside the range $\{1, \ldots, n\}$ (this happens close to the 4 corners of the given image), these 2D AR-BCs reduce to the one-dimensional case by making anti-reflection around the x axis and then around the y axis, separately. For instance, concerning the corner $(1, 1)$, we set $f_{1-j,1-l} = 4f_{1,1} - 2f_{1,l+1} - 2f_{j+1,1} + f_{j+1,l+1}$, for $1 \leq j, l \leq m$ (the idea around the other corners is similar). Regarding the 2D blurring, if the blurring function (PSF) h is strongly symmetric i.e., $h_{i,j} = h_{|i|,|j|}, \forall\, i, j \in \mathbb{Z}$, if $h_{i,j} = 0$ for $|i| > n-3$ or $|j| > n-3$ (support/degree condition), and h is normalized as $\sum_{i,j=-m}^{m} h_{i,j} = 1$, then the $n^2 \times n^2$ blurring matrix A, with anti-reflective boundary conditions, belongs to the algebra $\mathcal{S}_2$. With reference to (6) we have $\alpha = \beta = h_0 + 2\sum_{k=1}^{m} h_k$ where $h_k \in \mathcal{S}_1$ is the AR-BCs matrix related to the one-dimensional PSF $(h_{k,j})_{j=-m}^{m}$, $k = 0, \ldots, m$. Moreover, with reference to the the same notations for the h_k, $k = 0, \ldots, m$, and with reference to (6), we find $v_j = w_{n-1-j} = h_j + 2\sum_{k=j+1}^{m} h_k$ and M^* is a block $\tau_{n-2}^{(1)}$ whose block diagonal form is such that the j-th diagonal block is $h(x) = \alpha + 2\sum_{k=1}^{m} v_k \cos(kx) \in \mathcal{S}_1$ evaluated at $x_j^{(n)} = j\pi/(n-1)$, $j = 1, \ldots, n-2$ (see [23]). Therefore the spectrum of the blurring matrix A is given by 1 with multiplicity 4, by the values of $h_{(1)}(y) = h_{(1),0} + 2\sum_{k=1}^{m} h_{(1),k} \cos(ky)$ evaluated at $x_j^{(n)} = j\pi/(n-1)$, $j = 1, \ldots, n-2$, with multiplicity 2 and $h_{(1),k} = h_{0,k} + 2\sum_{j=1}^{m} h_{j,k}$, by the values of $h_{(2)}(x) = h_{(2),0} + 2\sum_{j=1}^{m} h_{(2),j} \cos(kx)$ evaluated at $x_j^{(n)} = j\pi/(n-1)$, $j = 1, \ldots, n-2$, with multiplicity 2 and $h_{(2),j} = h_{j,0} + 2\sum_{k=1}^{m} h_{j,k}$, and by the values of $h(x, y) = h_{0,0} + 2\sum_{j=1}^{m} h_{j,0} \cos(jx) + 2\sum_{k=1}^{m} h_{0,k} \cos(ky) + 4\sum_{j,k=1}^{m} h_{j,k} \cos(jx) \cos(ky)$ sampled

at $\left(x_j^{(n-2)}, x_k^{(n-2)}\right) = (j\pi/(n-1), k\pi/(n-1))$, $j,k = 1,\ldots,n-2$ (see [2]).

As a consequence of the block $\mathcal{S}_1$ structure of A and of the $\mathcal{S}_1$ structure of every block, it directly follows that each point-wise element of A has a computable expression which depends only on the entries $h_{i,j}$ of the blurring function. Hence the total complexity of writing down A from the PSF entries is within $O(n^2)$ additions.

3. Regularization and re-blurring

When the observed signal (or image) is noise free, then there is a substantial gain of the R-BCs with respect to both the periodic and zero Dirichlet BCs and, at the same time, there is a significant improvement of the AR-BCs with regard to the R-BCs (see [23, 10]). Since the de-convolution problem is ill-posed (components of the solution related to high frequency data errors are greatly amplified) regardless of the chosen BCs, it is evident that we have to regularize the problem. Two classical methods, i.e., Tikhonov regularization, with direct or iterative solution of the Tikhonov linear system, and regularizing iterative solvers, with early termination, for normal equations (CG [13] or Landweber method [3]) can be used. We observe that in both the cases, the coefficient matrix involves a shift of A^TA and that the righthand-side is given by $A^T\mathbf{g}$. Quite surprisingly, as already mentioned in the introduction, the AR-BCs may be spoiled by this approach at least for $d = 1$ and if we compute explicitly the matrix A^TA and the vector $A^T\mathbf{g}$, see [12]: more in detail, even in presence of a moderate noise and a strongly symmetric PSF, the accuracy of AR-BCs restorations becomes worse in some examples than the accuracy of R-BCs restorations. The reason of this fact relies upon the properties of the matrix A^T, and we give some insights in the following subsections.

3.1. The AR-BCs matrix and the re-blurring operator

A key point is that, for zero Dirichlet, periodic and reflective BCs, when the kernel h is symmetric, the matrix A^T is still a blurring operator since $A^T = A$, while, in the case of the AR-BCs matrix, A^T cannot be interpreted as a blurring operator. A (normalized) blurring operator is characterized by nonnegative coefficients such that every row sum is equal to 1 (and it is still acceptable if is not higher than 1): in the case of A^T with AR-BCs the row sum of the first and of the last row can be substantially bigger than 1. This means that modified signal $A^T\mathbf{g}$ may have artifacts at the borders and this seems to be a potential motivation for which a reduction of the reconstruction quality occurs.

Furthermore, the structure of the matrix A^TA is also spoiled and, in the case of images ($d = 2$) we lose the $O(n^2\log(n))$ computational cost for solving a generic system $A^TA\mathbf{x} = \mathbf{b}$. The reason of this negative fact is that $A^TA \notin \mathcal{S}_2$. More precisely, for $A \in \mathcal{S}_2$, we have

$$A^TA = \begin{bmatrix} \alpha & \mathbf{a}^T & \beta \\ \mathbf{a} & \tilde{M} & \mathbf{b} \\ \beta & \mathbf{b}^T & \gamma \end{bmatrix},$$

where $\mathbf{a} = (a_j)_{j=1}^{n-2}$, $\mathbf{b} = (b_j)_{j=1}^{n-2}$, $\tilde{M} = \left(\tilde{M}_{i,j}\right)_{i,j=1}^{n-2}$ with $a_j, b_j, \tilde{M}_{i,j}, \alpha, \beta, \gamma$, being expressible as the sum of a matrix belonging to $\mathcal{S}_1$ and a matrix of rank 2. Therefore since $\tilde{M}$ has external $\tau_{n-2}^{(1)}$ structure, it follows that A^TA can be written as the sum of a matrix in $\mathcal{S}_2$ and a matrix of rank proportional to n. The cost of solving such a type of linear systems is proportional to n^3 by using e.g. Shermann-Morrison formulae (which by the way can be numerically unstable [14]). Dealing with higher dimensions, the scenario is even worse [2], because in the d-dimensional

setting the solution of the normal equation linear system is asymptotic to $n^{3(d-1)}$, where n^d is the size of the matrix A. In order to overcome these problems (which arise only with the most precise AR-BCs for strongly symmetric PSFs), we replace A^T by A', where A' is the matrix obtained imposing the current BCs to the center-flipped PSF (that is, in the 2D case, to the PSF rotated by 180 degrees).

3.2. The case of strongly symmetric PSFs

For the sake of simplicity we first consider a strongly symmetric PSF so that the associated normal equations can be read as $A^2\mathbf{f} = A\mathbf{g}$, whenever zero Dirichlet, periodic or reflective BCs are considered. Therefore the observed image $\mathbf{g}$ is re-blurred. The re-blurring is the key of the success of classical regularization techniques (Tikhonov or CG, Landweber for the normal equations) since also the noise is blurred and this makes the contribution of the noise less evident. The latter informal explanation has to be made more precise. For the moment let us focus the attention on regularizing iterative solvers. It is self-evident that the solution of $A^2\mathbf{f} = A\mathbf{g}$ is the same as that of $A\mathbf{f} = \mathbf{g}$ if A is nonsingular, and therefore, after the filtering step due to the multiplication by A, the solution of the linear system will undo any filtering: in other words the reconstruction will de-blur the blurred vector $A\mathbf{g}$. However, the above reasoning holds only if the solution of the system is done algebraically, while any regularizing iterative solver is characterized by the use of an appropriate early termination technique: in this sense the solution of $A^2\mathbf{f} = A\mathbf{g}$ with best termination is not the same as the solution of $A\mathbf{f} = \mathbf{g}$ with best termination. Indeed the main point of methods such as Landweber or CG is that the reconstruction is faster in the subspace related to non-vanishing eigenvalues and is slower in the complementary subspace. Let $\mathcal{L}$ be the space generated by the eigenvectors of A related to small eigenvalues. In the case where $\mathcal{L}$ largely intersects the noisy space while the signal has no significant components in $\mathcal{L}$, the multiplication by A implies that the iterative solver will delay the reconstruction of the noise and of the portion of the signal in high frequency. Indeed, by early termination, we are equally sacrificing the reconstruction of the signal in high frequency and the reconstruction of the noise in high frequency: here the a-priori assumption on the frequency decomposition of the involved objects comes into the play. Just by an example, if in high frequency there is the 10% of the signal and there is the 60% of the noise, then by re-blurring and early termination we are sacrificing a little portion of the signal and a much higher portion of the noise contribution (all these informal arguments can be turned into formal, by employing a classical Fourier Analysis). In conclusion, the best termination will occur later and the reconstructed object will contain a larger portion of the true object. In this direction it is interesting to notice that also the use of a different blurring operator B could be considered (see [12, Subsection 3.1]), leading to some improvement in specific cases (see [12, Subsection 4.2, Table 8]). Of course this more general approach is very delicate: if the vanishing space (or the kernel) of B is too large then also the reconstruction of the true object could be excessively delayed and, as a consequence, the overall quality could be spoiled; moreover in general we loose the symmetry of BA and this can lead to a less regular behavior of many iterative solvers. Another evidence of the above reasoning is the better behavior of the normal equation approach versus the Riley approach [20], when A is ill-conditioned and symmetric positive definite. In fact, all the numerics uniformly show that:

- the solution of $(A^2 + \mu\mathcal{T}^2)\mathbf{f} = A\mathbf{g}$, $\mathcal{T}$ symmetric positive definite, with best parameter is always better than the solution of $(A + \mu\mathcal{T})\mathbf{f} = \mathbf{g}$ (Riley) with best parameter;
- the solution of $A^2\mathbf{f} = A\mathbf{g}$ by CG with best termination is always better than the solution

of $A\mathbf{f} = \mathbf{g}$ by CG with best termination.

With respect to the second item, we notice that the two systems $A^2\mathbf{f} = A\mathbf{g}$ and $A\mathbf{f} = \mathbf{g}$ are algebraically equivalent: the first represents the minimization of the functional $\|A\mathbf{f}-\mathbf{g}\|_2^2$ while the second represents the minimization of the (equivalent) functional $\|A^{1/2}\mathbf{f} - A^{-1/2}\mathbf{g}\|_2^2$ so that the first can be considered the blurred version of the second and in fact the first approach is uniformly better than the second. On these grounds, in the case of AR-BCs, since $A^T \neq A$, we can replace A^T by A which is again a low-pass filter (see [12]). In this way, we overcome also the computational problems since A^2 belongs to the $\mathcal{S}_d$ algebra.

3.3. The case of nonsymmetric PSFs

In order to provide a general re-blurring approach also in the case of nonsymmetric PSFs, we consider the correlation operation instead of the transposition (see [7]). In the discrete 2D case, the correlation performs the same operation of the convolution, but rotating the mask (the PSF in our case) of 180 degrees. Moreover we note that in the continuous case over an infinite domain, the correlation and the adjoint are exactly the same operation, provided that the convolution kernel is real. Indeed, let K be the convolution operator with shift-invariant kernel $k(s)$, then

$$[Kf](x) = \int k(x-y)f(y)\mathrm{d}y.$$

Since the PSF (and then k) is real (and then real-valued), the adjoint operator K^* is

$$[K^*f](x) = \int k(y-x)f(y)\mathrm{d}y.$$

which is a correlation operator. We remark that here the convolution and the correlation use the same kernel except for the sign of the variable (i.e., $k(\mathbf{s})$ vs $k(-\mathbf{s})$), and, in the 2D case, the change of sign in the variable $\mathbf{s}$ of the kernel can be viewed as a 180 degrees rotation of the PSF mask.

By virtue of these arguments, in order to overcome the problems arising with the normal equations approach for AR-BCs 2D restorations, we propose to replace A^T by A' (the re-blurring matrix), where A' is the matrix obtained imposing the BCs to the PSF rotated by 180 degrees. Using Matlab notation, if H is a $q \times q$ PSF, its 180 degrees rotated version is $H' = \mathrm{fliplr}(\mathrm{flipud}(H)) = J_q H J_q$, where J_q is the flip matrix defined as $[J_q]_{i,j} = 1$ if $i+j = q+1$ for $i, j = 1, \ldots, q$, and zero otherwise. For a d-dimensional problem, A' is obtained imposing the BCs to the PSF flipped with respect to the origin, or, in other words, to the new PSF where all the coefficients are flipped with respect to every variable.

In this way A' has the same computational properties of A and it is certainly a low pass filter. In the re-blurring approach the normal equations are replaced by

$$A'A\mathbf{f} = A'\mathbf{g}. \tag{7}$$

Furthermore, using the Tikhonov regularization, we propose to use

$$\left[A'A + \mu\mathcal{T}'\mathcal{T}\right]\mathbf{f} = A'\mathbf{g}, \tag{8}$$

with $\mathcal{T}$ being any discrete differential operator with AR-BCs. From the viewpoint of the modeler, the previous considerations can be summarized in the following motivation. The image restoration problem is the restriction in the FOV of an infinite dimensional problem. We can follow two ways to design the linear system to solve:

(i) to impose BCs and then to look at a least-squares solution,

(ii) to formulate a least-squares solution on the infinite dimensional problem, and then to impose the BCs to the two infinite dimensional operators K and K^*, separately.

A third possibility is to formulate a least-squares solution on the infinite dimensional problem, and then to impose the BCs to this minimum problem: a difficulty in this case is that, even without noise, the resulting system is not equivalent in an algebraic sense to the original equations $A\mathbf{f} = \mathbf{g}$.

In the first case we resort to the normal equations in the finite dimensional space. On the contrary, in the second case we apply the BCs to K and K^* in the infinite dimensional normal equations (where the adjoint operator K^* performs a correlation operation) and then we obtain (7). More precisely, the discretization of K and K^* in the continuous equation $K^*Kf = K^*g$ with any fixed BCs gives (7).

3.4. Linear algebra issues

We note that in the 1D case $A'_n = J_n A_n J_n$. In the d-dimensional case, let $n = (n_1, n_2, \ldots, n_d)$ be the partial dimensions of the problem, whose total size is $\prod_{i=1}^{d} n_i$. By flipping each variable, we obtain

$$A'_n = J_n A_n J_n, \qquad J_n = \bigotimes_{i=1}^{d} J_{n_i}. \tag{9}$$

For the analysis of properties of the re-blurring scheme (7) with respect to all the different BCs, we now study the discretization of the continuous operator K. Let us consider the Toeplitz d-level matrix $T_n(\phi)$ of partial dimensions $n = (n_1, \ldots, n_d) \in \mathbb{N}_+^d$ and generating function ϕ [9], which is defined as

$$T_n(\phi) = \sum_{|j| \le n-e} a_j Z_n^{[j]} = \sum_{|j_1| < n_1} \cdots \sum_{|j_d| < n_d} a_{(j_1,\ldots,j_d)} Z_{n_1}^{[j_1]} \otimes \ldots \otimes Z_{n_d}^{[j_d]}$$

($e = (1, \ldots, 1) \in \mathbb{N}_+^d$) by means of the Fourier coefficients of ϕ

$$a_k = \frac{1}{(2\pi)^d} \int_{[-\pi,\pi]^d} \phi(x) \mathrm{e}^{-\mathbf{i}\langle k|x\rangle} \mathrm{d}x, \qquad \mathbf{i}^2 = -1, \qquad k \in \mathbb{Z}^d. \tag{10}$$

Here $\langle k|x\rangle = \sum_{i=1}^{d} k_i x_i$ and for $j \in \mathbb{Z}$, $m \in N_+$, $Z_m^{[j]} \in \mathbb{R}^{m\times m}$ is the matrix whose (s,r)-th entry is 1 if $s - r = j$, and 0 elsewhere. As it is well-known for multilevel Toeplitz matrices $T_n^H(\phi) = T_n(\overline{\phi})$, where $\overline{\phi}$ is the conjugate of the function ϕ, and the Fourier coefficients of $\overline{\phi}$ are the same of ϕ, but conjugated and flipped. Moreover, since $T_n(\overline{\phi}) = J_n \overline{T_n(\phi)} J_n$, if $A_n = T_n(\phi)$ is real then $A_n^T = J_n A_n J_n = A'_n$. This means that for Dirichlet BCs (D-BCs) and periodic BCs (P-BCs) the re-blurring approach is exactly equal to the classical normal equations approach, since in these two cases the corresponding blurring matrix A_n is multilevel Toeplitz: indeed, concerning P-BCs, we notice that the resulting multilevel circulant structure is a special instance of the multilevel Toeplitz case. Unfortunately, in the case of Hankel matrices (or multilevel mixed Toeplitz-Hankel matrices with at least one Hankel level) this is no longer true in general. However, a sufficient and necessary condition to have $A'_n = A_n^T$ is $J_n A_n = (J_n A_n)^T$ (or equivalently $A_n J_n = (A_n J_n)^T$), which is a multilevel antidiagonal symmetry called persymmetry. Therefore in the case of R-BCs, where the matrix A_n involves nested Hankel parts, in general $A'_n \neq A_n^T$, while $A'_n = A_n^T$ only when the PSF is strongly symmetric since in this case $J_n A_n = (J_n A_n)^T$. Dealing with the AR-BCs, the situation is even more involved, since $A'_n \neq A_n^T$ also for strongly symmetric PSFs, owing to the low-rank correction term. Hence, we can state that the re-blurring is a new proposal not only for

the AR-BCs, but also for all those BCs for which $J_nA_n \neq (J_nA_n)^T$. As a nontrivial and unexpected example, it is important to stress that the imposition of R-BCs with non-strongly symmetric PSFs implies $J_nA_n \neq (J_nA_n)^T$ i.e. $A'_n \neq A_n^T$.

3.5. Computational issues

We provide now a computational motivation for the choice of using A' as an alternative to A^T: A' is the usual operation which has to be implemented to perform the adjoint operation in the Fourier domain. Indeed, the convolution with prescribed BCs can be implemented by first enlarging the image according to the considered BCs and then by computing the matrix vector product by a simple circular convolution operation, see [17]. More precisely, let X and H be two matrices such that X represents an $n \times n$ image and H is the discrete $q \times q$ 2D PSF, $q = 2m + 1$, which leads to the matrix blurring A. By using the Matlab notation $\mathbf{x} = X(:)$ (i.e., the vector $\mathbf{x}$ is the column-stacked version of X), the product $A\mathbf{x}$ in the 2D case can be implemented

(i) by using an enlarged image $\tilde{X}$, which is the $(n + q - 1) \times (n + q - 1)$ image X extended at the boundaries according to the imposed BCs,

(ii) computing $H * \tilde{X}$, where the symbol "$*$" denotes the circular convolution operator (H should be zero padded to have the same size of $\tilde{X}$),

(iii) and then taking the inner part of the result having the same size of X.

The circular convolution can be computed using the 2D discrete Fourier transform (DFT2) and its inverse (IDFT2), since we have

$$H * \tilde{X} = \mathrm{IDFT2}(\mathrm{DFT2}(H) \odot \mathrm{DFT2}(\tilde{X})), \tag{11}$$

where "$\odot$" is the componentwise product. If $\mathcal{C}_k(f)$ denotes the block circulant matrix with circulant blocks, of block size k with blocks of size k and generating function f, then (11) represents the same operation as $\mathcal{C}_{n+q-1}(\phi)\tilde{\mathbf{x}}$, where $\tilde{\mathbf{x}} = \tilde{X}(:)$ (according to a 2D ordering). Conversely, it is well known that the operation corresponding to the product with the adjoint operator, in the Fourier domain gives rise to

$$Y = H' * \tilde{X} = \mathrm{IDFT2}(\overline{\mathrm{DFT2}(H)} \odot \mathrm{DFT2}(\tilde{X})), \quad H'_{i,j} = H_{-i,-j},\ i, j \in \mathbb{Z},$$

where the overline symbol denotes the complex conjugation. As a result, since the transform $H \mapsto H'$ is equivalent to the transform $\phi \mapsto \overline{\phi}$ (because $\phi(x, y) = \sum_{i,j\in\mathbb{Z}} H_{i,j}\mathrm{e}^{\mathbf{i}\langle(i,j)|(x,y)\rangle}$), and since $\mathcal{C}_{n+q-1}(\overline{\phi}) = \mathcal{C}^T_{n+q-1}(\phi)$, if $\mathbf{y} = Y(:)$, then it follows that $\mathbf{y} = \mathcal{C}^T_{n+q-1}(\phi)\tilde{\mathbf{x}}$. Therefore, for any of the considered BCs, the inner part of $\mathbf{y}$ is exactly $A'\mathbf{x}$. Here it is worthwhile to specify exactly what we mean for inner part: if the vector $\mathbf{y}$ is partitioned in $n + q - 1$ blocks of size $n + q - 1$, $q = 2m + 1$, then for inner part we mean that we are excluding the first and the last m blocks and, in any of the remaining blocks, we are deleting the first and the last m entries. More generally, if the PSF is arbitrary (e.g. nonsymmetric) i.e. the nonzero coefficients of the PSF have first index belonging to $[-m_1^-, m_1^+]$ and second index in the range $[-m_2^-, m_2^+]$, then we have to delete the first m_1^- and the last m_1^+ blocks and, in any of the other blocks, we have to exclude the first m_2^- and the last m_2^+ entries.

Since the DFT and its inverse can be computed in $O(n^2 \log(n))$ arithmetic operations using FFTs, the previous approach is implemented in the Matlab toolbox RestoreTools [17]. We have added the AR-BCs in such a toolbox for the matrix vector product, suitable for iterative regularizing methods. This code has been used for the

numerical tests of Section 4 and it is downloadable from the home-page "http://scienze-como.uninsubria.it/mdonatelli/software.html".

3.6. Further spectral and computational features of the re-blurring operator

In this subsection, we sketch few spectral and computational properties of the re-blurring matrix A' in the case of AR-BCs.

As already observed, the 180 degrees rotation of the PSF (i.e. the conjugation of the generating function) corresponds to a permutation of rows and columns of A, which is obtained by (9). Hence the eigenvalues of A' are the same of A (A' and A are similar, see [14]) and in the strongly symmetric case, since $A' = A \in \mathcal{S}_d$ and the eigenvalues of A are real, all eigenvalues of $A'A = A^2$ are nonnegative. Consequently, if also $\mathcal{T}', \mathcal{T} \in \mathcal{S}_d$, the cost of solving the Tikhonov-like linear system (8) is proportional to $n^d \log(n)$ thanks to Theorem 2.1. In addition, since any AR-BCs matrix with strongly symmetric PSF, satisfying a proper support/degree condition (see Section 2) is diagonalizable, it follows that $A'A = A^2$ is similar to a positive definite (or at least nonnegative definite) matrix: we stress that the latter fact could be helpful in proving the convergence of the standard CG to the re-blurred system (7). In the general case, the anti-reflective matrix A has a multilevel mixed Toeplitz-Hankel structure plus a correction term R of rank of the order n^{d-1} if each partial dimension is equal to n, moreover $JRJ \neq R^T$. Therefore the antisymmetric part of $A'A$ (i.e. $(A'A - (A'A)^T)/2$) has again rank of order at most n^{d-1} since $A'A \in \mathcal{S}_d$. The robustness of CG with respect to special structured (small rank) perturbations in the symmetry is well-known, thus, thanks to the previous remarks, it may be reasonable to expect that the CG works fine for solving (7). This is exactly what happens in all our numerical experiments reported and discussed in the subsequent Section 4. However, a formal and complete proof of the applicability of the CG to the linear system (7) and a deeper analysis of the eigenvalues/eigenvectors structure of the associated matrix $A'A$ are still open problems and will be considered in future researches.

4. Numerical experiments

In our numerical experiments we use Matlab 7.0 and the toolbox RestoreTools [17] suitably extended for dealing with AR-BCs. The relative restoration error (RRE) is $\|\hat{\mathbf{f}} - \mathbf{f}\|_2/\|\mathbf{f}\|_2$, where $\hat{\mathbf{f}}$ is the computed approximation of the true image $\mathbf{f}$. The signal-to-noise ratio (SNR) is computed as $20 \log_{10} \|\mathbf{g}_b\|_2/||\boldsymbol{\nu}||_2$, where $\mathbf{g}_b$ is the blurred image without noise and $\boldsymbol{\nu}$ is the noise vector [3].

4.1. Comparison between normal equations and re-blurring

The first test is an example of nonsymmetric PSF, whose aim is to give evidence of the effectiveness of the re-blurring approach with noisy data (in the case of R-BCs as well). We consider the true image, the PSF, and the blurred image in Figure 1. In the true image the FOV is delimited by white lines. In Table 1 we report the RREs related to different SNRs of Gaussian noise for the CG regularization. We note that the two approaches give comparable RREs. On the other hand, we should recall the computational gain in the use of the re-blurring strategy, which is also increased thanks to a faster convergence of the CG method. However, it is clear that a more complete analysis and further comparisons are required in the future, especially concerning the restoration quality of the two strategies.

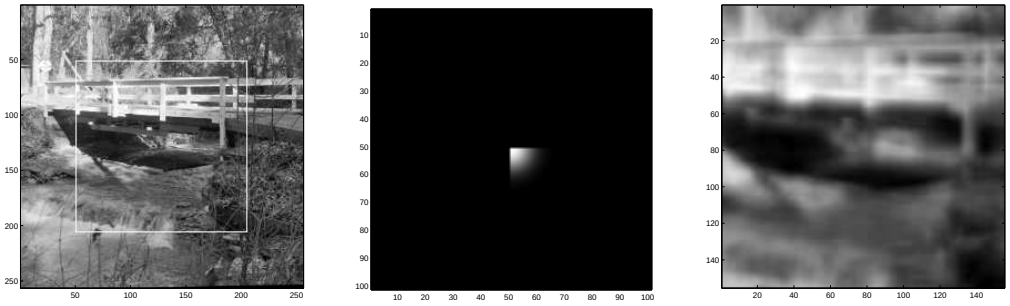

True image PSF Blurred image

Figure 1. True image, PSF, and blurred image without noise.

Table 1. RREs with CG regularization.

	Normal Equations		Re-blurring	
SNR	Reflective	Antireflective	Reflective	Antireflective
∞ (0% noise)	0.1183	0.0276	0.1189	0.0280
50	0.1263	0.0712	0.1259	0.0719
40	0.1290	0.0962	0.1289	0.0988
30	0.1441	0.1315	0.1440	0.1360
20	0.1975	0.1946	0.1967	0.1961

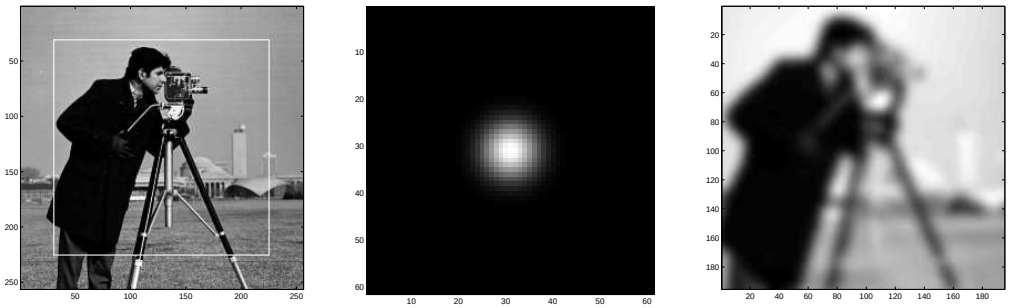

True image Gaussian PSF Blurred image

Figure 2. Test I: true image, Gaussian PSF, and the blurred image without noise.

4.2. Re-blurring and CG regularization

In the following tests, the re-blurring strategy will be applied with R-BCs and AR-BCs when the PSF is not necessarily strongly symmetric. Indeed, in the case of D-BCs and P-BCs, the re-blurring approach is equal to the classical normal equations, while, in the case of R-BCs and AR-BCs, this is no longer true in general.

We consider provide two problems using iterative regularization by CG.

Test I: *Cameraman*

The first test is reported in Figure 2. The true image is a cameraman and the 61×61 PSF is associated with a Gaussian distribution in the square domain $[-30, 30] \times [-30, 30]$, with variance equal to four. We add a Gaussian noise.

Test II: *Astronomy*

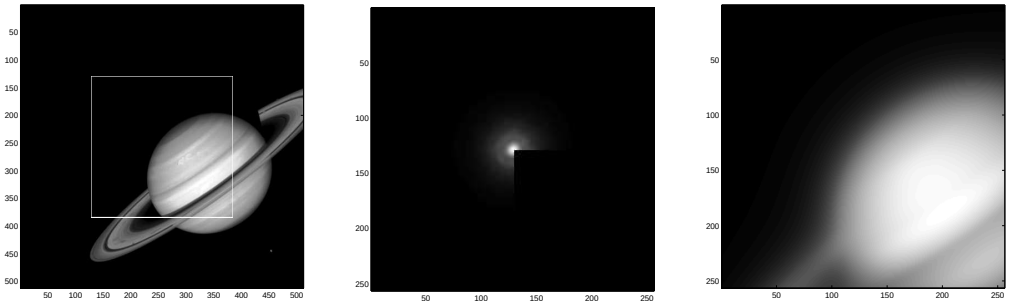

True image PSF Blurred image

Figure 3. Test II: true image, PSF, and the blurred image without noise.

Table 2. Test I: best RREs and L^2 norm of the residuals for CG with re-blurring varying the SNR (SNR $= \infty$ means 0% of noise).

	Relative restoration errors			L^2 norm of the residuals ($\|\mathbf{g} - A\hat{\mathbf{f}}\|_2^2$)		
SNR	Periodic	Reflective	Anti-Reflective	Periodic	Reflective	Anti-Reflective
∞	0.2275	0.1993	0.1831	1.2363	0.0113	0.0004
50	0.2276	0.1996	0.1850	1.2728	0.0480	0.0374
40	0.2278	0.2007	0.1921	1.6078	0.3766	0.3654
30	0.2300	0.2088	0.2051	4.9395	3.7346	3.7133
20	0.2487	0.2382	0.2378	38.2357	37.2100	37.2149
10	0.3836	0.3814	0.3823	379.2445	376.0303	376.0419

We are dealing with a strongly non symmetric portion of an experimental 256×256 PSF developed by US Air Force Phillips Laboratory, Lasers and Imaging Directorate, Kirtland Air Force Base, New Mexico, widely used in literature (see e.g. [18, 19]). The true object is the image of Saturno in Figure 3; a Poissonian noise is added, as it is customary when dealing with astronomical images.

We show the results corresponding only to P-BCs, R-BCs and AR-BCs. For shortness, we do not report the reconstructions coming from D-BCs, since the related restorations are usually not better than those with P-BCs.

Tables 2–3 show the best RREs for various levels of noise. In Table 2 we also report the L^2 norm of the residuals i.e. $\|\mathbf{g} - A\hat{\mathbf{f}}\|_2^2$, where $\mathbf{g}$ is the observed image, $\hat{\mathbf{f}}$ is the computed approximation, and A is the coefficient matrix constructed according to the considered BCs: the latter measure is the sum of square errors and it represents, up to the scaling of the variance, the χ^2 statistical measure of the error. As already pointed out, the choice of the BCs is important mainly for low levels of noise, that is, for high values of SNR. Indeed, in the last row of these tables (SNR $= 10$), the errors due to noise start to dominate the restoration process and therefore the choice of particular BCs is not relevant for the restoration accuracy. In the other rows, where the noise is lower, the choice of the BCs becomes crucial. In particular, the AR-BCs improve substantially the quality of the restorations with respect to the others BCs. This is especially evident in Test II (see Table 3). The reason of the observed high improvement is due to the shape of the PSF, since, basically, the more the support of the PSF

Table 3. Test II: best RREs for CG with re-blurring varying the SNR (SNR = ∞ means 0% of noise) within 200 iterations.

SNR	Periodic	Reflective	Anti-Reflective
∞	0.2353	0.1521	0.0816
50	0.2353	0.1521	0.0819
40	0.2356	0.1525	0.0837
30	0.2371	0.1552	0.1063
20	0.2529	0.1807	0.1553
10	0.3717	0.3336	0.3319

is large, the more the ringing effects (and hence the BCs) become dominating.

To emphasize the quality of the restored images, we consider the reconstruction in the case of Test I for a fixed SNR equal to 40. In Figure 4 we report the restored images and in Figure 5 the residuals of the computed solutions for each pixel divided by the variance of the noise. This last one should have a normal distribution in the case of a good restoration since we add a Gaussian noise. In Figure 4 is evident the reduction of the ringing effects passing from P-BCs to R-BCs (ringings such as the horizontal white line on the top and the horizontal black line on the bottom disappear) and from R-BCs to AR-BCs (ringings such as the two vertical white lines in the bottom left disappear). Indeed, in the same figure we note an higher level of detail in the case of AR-BCs, especially concerning the face of the cameramen. The image restored with R-BCs is smoother when compared with the restored one with AR-BCs, where we can see the "freckles" effect, typical of the L^2 norm restoration. Indeed the CGLS method computes the least-squares solution that is well-known to be affected by such a phenomenon [16]. When passing to the R-BCs, the considered effect is less evident: indeed it seems that the slightly greater ringing effects smooth the image reducing the "freckles", but also reducing some details like, e.g., the eye of the cameraman. The previous comments suggest that using AR-BCs in connection with regularization methods related to other norms, like the Total Variation [22], could lead to a reconstruction with sharper edges. In Figure 5 we observe a normal distribution of the scaled residuals only with the AR-BCs, while, also with the R-BCs, some further errors corresponding to the ringing effects emerge at the boundary and at the edges of the image: this means that the imposition of the R-BCs is not good enough as model at least for this example. On the other hand, with the AR-BCs, this kind of error seems to disappear and the scaled residual seems to follows a normal distribution. This confirms the goodness of the restoration obtained with the AR-BCs.

Two convergence histories, i.e., the RREs at any iteration, are plotted in Figures 6 for two different values of the SNR. It should be stressed that the AR-BCs give the best results and the lowest level of RRE. Such behavior is again more evident considering Test II. Indeed, in such case the RREs with AR-BCs continue to decrease even after the first 200 iterations. On the other hand, the restorations with R-BCs start to deteriorate after the very first iterations. In addition, we notice that AR-BCs curves are in general quite flat. This is a very useful feature since the estimation of the optimal stopping value, which is well-known to be a crucial and difficult task, can be done with low precision. Indeed, in order to stress the applicability of the AR-BCs to real problems, we consider for the Test I the discrepancy principle widely used with iterative methods [13]. Since we know the L^2 norm of the error, we stop the CG when

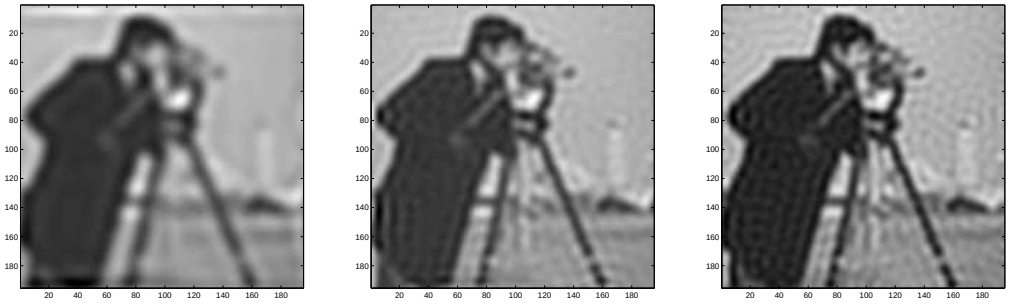

Periodic Reflective Anti-reflective

Figure 4. Restored images with SNR = 40.

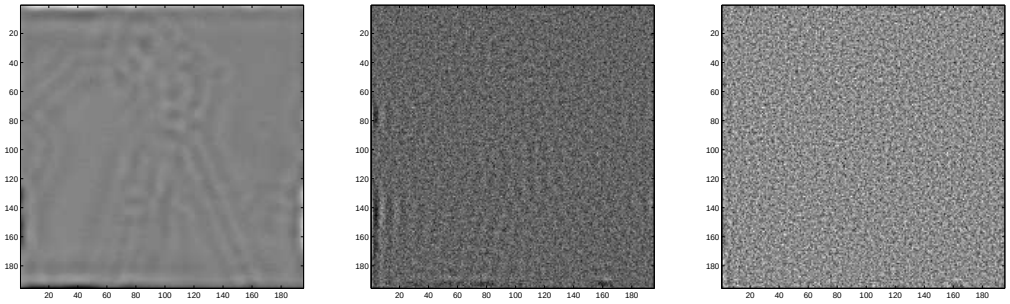

Periodic Reflective Anti-reflective

Figure 5. Residuals divided by the variance of the noise for the restored images with SNR = 40.

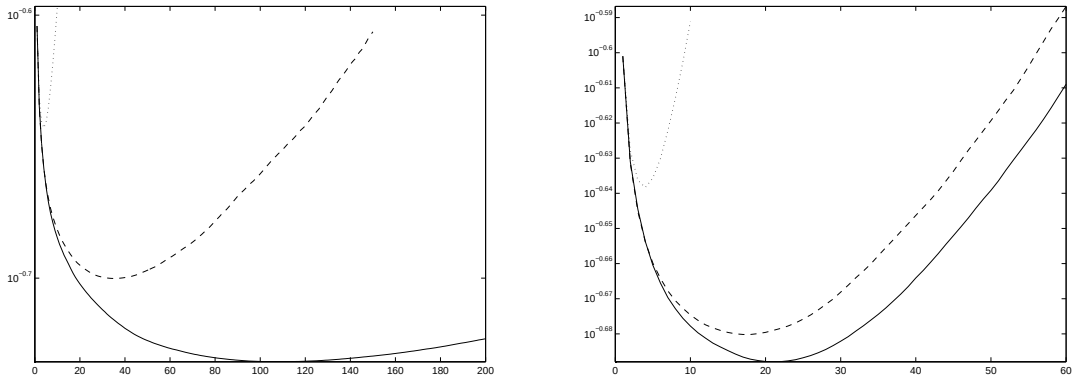

SNR= 50 SNR= 30

Figure 6. Test I: RRE at each CG iteration with different BCs: ·····Periodic, – – –Reflective ——Antireflective.

the L^2 norm of the residual becomes lower then the L^2 norm of the error. Such a criterium seems to work quite well for the AR-BCs as we can see in Figure 7. The restored images are good enough with respect to the optimal solution and also the stopping iteration, at least in this example, is close to the optimal one. On the other hand such criterium is not always effective for the other BCs in this example. For instance the stopping iteration for R-BCs is greater than 1000 in the case of SNR = 50 and it is 13 for SNR = 30. However an analysis of the stopping criterium, in connection with AR-BCs, should be further investigated in the

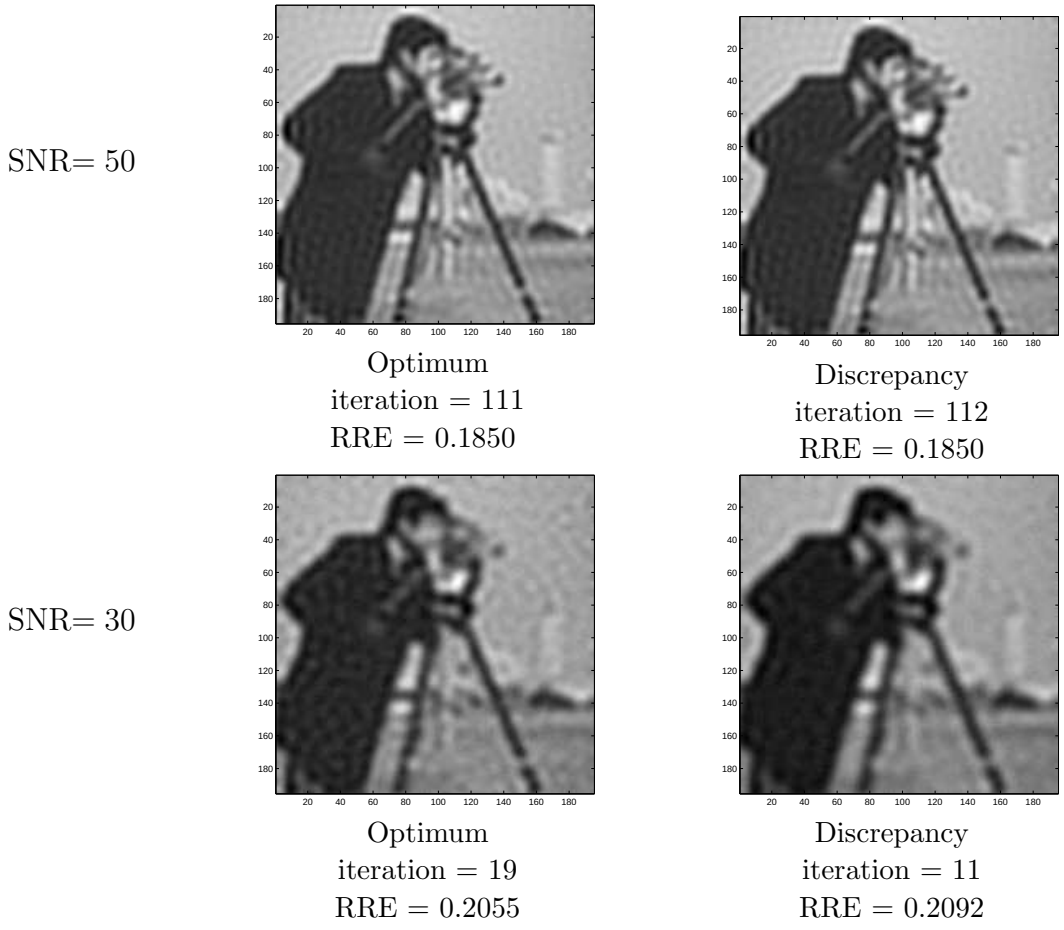

Figure 7. Discrepancy principle: images restored at the optimum value iteration and at which computed with the discrepancy principle.

future.

Finally, we remark that also for Test II the CG applied to the linear system (7) works without breakdown, both with R-BCs and AR-BCs. Therefore, it is possible that the applicability of the CG to (7) is a general property, which does not depend on the particular choice of the boundary conditions.

4.3. Re-blurring and Tikhonov regularization

The PSF of Test I is strongly symmetric. Therefore, in the R-BCs case, the matrix A can be diagonalized by the discrete cosine transform (DCT) [19]. The considered property allows to solve the Tikhonov linear system $(A^TA + \mu I)\mathbf{f} = A^T\mathbf{g}$ with only three two-level DCTs of size n^2. In the AR-BCs case, as already observed, we resort to the re-blurring and then we compute the modified Tikhonov solution $\mathbf{f}$ defined by $(A'A+\mu I)\mathbf{f} = A'\mathbf{g}$. Thanks to Theorem 2.1, the latter linear system can be solved with few two-level discrete sine transforms of size $(n-2)^2$ plus some lower order computations. Therefore the two following approaches:

(i) to solve $(A^TA + \mu I)\mathbf{f} = A^T\mathbf{g}$ with R-BCs,

(ii) to solve $(A'A + \mu I)\mathbf{f} = A'\mathbf{g}$ with AR-BCs,

Table 4. Tikhonov: best RREs for Tikhonov comparing reflective BCs (using normal equations) with antireflective BCs (using re-blurring) varying the SNR (SNR = ∞ means 0% of noise).

SNR	Reflective $(A^TA + \mu I)\mathbf{f} = A^T\mathbf{g}$	Anti-Reflective $(A'A + \mu I)\mathbf{f} = A'\mathbf{g}$
∞	0.1974	0.1815
50	0.1974	0.1839
40	0.1980	0.1900
30	0.2056	0.2031
20	0.2174	0.2175
10	0.2458	0.2500

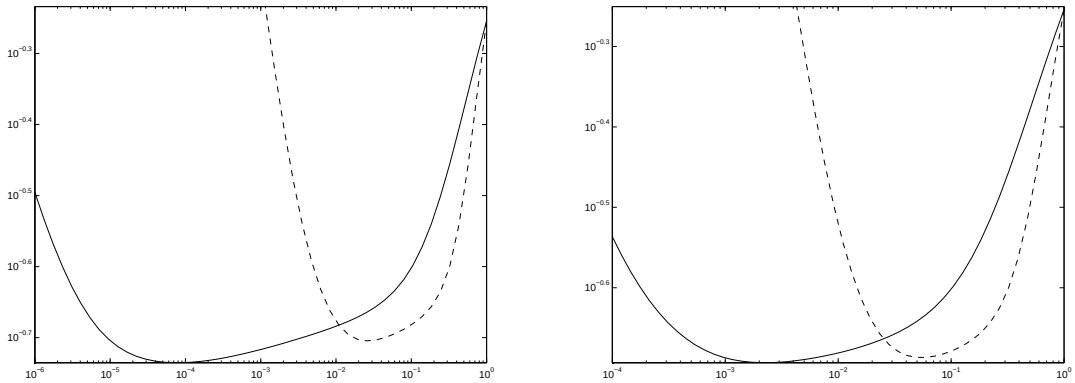

SNR= 50 SNR= 30

Figure 8. Tikhonov: RRE vs μ: – – –Reflective ——Antireflective.

have a comparable computational cost. The RREs in Table 4 confirm the similar behavior emphasized by Table 2 with the CG regularization. Furthermore, analogously to what was observed for CG regularization in Figure 6, the choice of the regularization parameter μ is less crucial with AR-BCs than with R-BCs. Indeed, in Figure 8 the curve of the RRE vs the parameter μ with AR-BCs is much flatter around the minimum than with R-BCs.

5. Conclusions

In this paper, a new basic modification, called re-blurring, of the normal equations (both for the Tikhonov regularized equation to be solved exactly and for the standard normal equations to be solved by CG with early termination) is proposed for the solution of de-convolution problems. Thanks to the filtering properties of any blurring operator in the sense of Subsections 3.1-3.3, by using this modification, the anti-reflective choice becomes again convenient among all the considered BCs even in presence of high levels of noise and nonsymmetric PSFs. We have shown that the new formulation allows us to overcome the computational difficulties due to the role of the low rank term in the product A^TA of the blurring operator A related to the AR-BCs. By doing so, the restored d-dimensional object can be computed in $O(n^d \log(n))$ real operations by using few fast j-level FSTs with $j \leq d$, if the PSF is strongly symmetric [2]. In particular, also in the nonsymmetric case, the proposed technique allows

- very high reduction of the ringing effects in the reconstructed images even with respect to the R-BCs;
- fast computation, i.e. $O(n^d \log(n))$ arithmetic operations in a d-dimensional setting, if we use iterative solvers where only fast matrix-vector products are required;
- easier choice of the regularization parameter: in other words, it is simpler to determine a quasi-optimal iteration where the iterations have to be stopped.

Under these considerations, it should be of interest to extend the technique to real applications such as LBT or 3D microscopy (see e.g. [11]). Future works will be addressed to these real applications, since the properties of the PSF (which is close to be symmetric, see e.g. [1]) and the features of the images (which are nonzero nearby the boarders, see e.g. [1]) seem to fit quite well with the proposed AR-BCs re-blurring technique. A theoretical analysis of the re-blurring strategy will be useful, in connection with the relations between the correlation and the transposition operators. Moreover, we would like to prove that the CG applied to a linear systems with coefficient matrix $A'A$ does not have breakdown also in the general case of nonsymmetric PSFs: in this respect, we stress that all the experimentations seem to bode well, since we did not encounter any algorithmic problem with CG so far. Finally a more detailed analysis of the stopping criterium for the AR-BCs should be investigated.

Acknowledgements Warm thanks to Jim Nagy and to the referees for very pertinent and useful remarks. The work of all the authors was partially supported by MIUR, grant number 2004015437.

References

[1] B. Anconelli, M. Bertero, P. Boccacci, M. Carbillet, and H. Lanteri 2005 *Reduction of boundary effects in multiple image deconvolution with an application to LBT LINC-NIRVANA*, Astron. Astrophys., **448** pp. 1217–1224.

[2] A. Aricò, M. Donatelli, and S. Serra Capizzano 2006 *The anti-reflective algebra: structural and computational analysis with application to image deblurring and denoising*, manuscript.

[3] M. Bertero and P. Boccacci 1998 *Introduction to Inverse Problems in Imaging*, Inst. of Physics Publ. London, UK.

[4] M. Bertero and P. Boccacci 2000 *Image restoration for Large Binocular Telescope (LBT)*, Astron. Astrophys. Suppl. Ser. **147** pp. 323–332.

[5] M. Bertero and P. Boccacci 2005 *A simple method for the reduction of the boundary effects in the Richardson-Lucy approach to image deconvolution*, Astron. Astrophys. **437** pp. 369–374.

[6] D. Bini and M. Capovani 1983 *Spectral and computational properties of band symmetric Toeplitz matrices*, Linear Algebra Appl. **52/53** pp. 99–125.

[7] E. O. Brigham 1988 *The Fast Fourier Transform and Applications*, Prentice Hall, Englewood Cliffs, NJ.

[8] D. Calvetti and E. Someralo 2005 *Statistical elimination of boundary artefacts in image deblurring*, Inverse Problems **21** pp. 1697–1714.

[9] R. H. Chan and M. Ng 1996 *Conjugate gradient methods for Toeplitz systems*, SIAM Rev. **38** pp. 427–482.

[10] M. Donatelli, C. Estatico, J. Nagy, L. Perrone, and S. Serra Capizzano 2003 *Anti-reflective boundary conditions and fast 2D deblurring models*, Proceeding to SPIE's 48th Annual Meeting, San Diego, CA USA, F. Luk Ed, **5205** pp. 380–389.

[11] M. Donatelli, C. Estatico, and S. Serra Capizzano 2005 *Boundary conditions and multiple-image re-blurring: the LBT case*, J. Comput. Appl. Math., in press.

[12] M. Donatelli and S. Serra Capizzano 2005 *Anti-reflective boundary conditions and re-blurring*, Inverse Problems **21** pp. 169–182.

[13] H. Engl, M. Hanke, and A. Neubauer 1996 *Regularization of Inverse Problems*, Kluwer Academic Publishers, Dordrecht, The Netherlands.

[14] G. Golub and C. Van Loan 1983 *Matrix Computations*, The Johns Hopkins University Press, Baltimore.

[15] M. Hanke and J. Nagy, *Restoration of atmospherically blurred images by symmetric indefinite conjugate gradient technique*, Inverse Problems, 12, pp. 157–173, 1996.

[16] P. C. Hansen, J. Nagy, and D. P. O'Leary 2006 *Deblurring Images Matrices, Spectra and Filtering*, SIAM Pulications, Philadelphia.

[17] J. Nagy, K. Palmer, and L. Perrone 2002 *RestoreTools: An object oriented Matlab package for image restoration*, http://www.mathcs.emory.edu/∼nagy/RestoreTools.

[18] J. Nagy, K. Palmer, and L. Perrone 2004 *Iterative methods for image deblurring: a Matlab object-oriented approach*, Numer. Algorithms **36** pp. 73–93.

[19] M. Ng, R. H. Chan, and W. C. Tang 1999 *A fast algorithm for deblurring models with Neumann boundary conditions*, SIAM J. Sci. Comput. **21** pp. 851–866.

[20] J. D. Riley 1963, *Solving systems of linear equations with a positive definite, symmetric, but possibly ill-conditioned matrix*, Math. Tables Aids Comput. **9** pp. 96–101, English transl. Dokl. Akad. Nauk. SSSR **151** (1955) pp. 501–504.

[21] T. P. Ryan, 1997 *Modern regression methods*, John Wiley & Sons Inc., New York.

[22] L. Rudin, S. Osher, and E. Fatemi, 1992 *Nonlinear total variation based noise removal algorithms*, Physica. D, **60** pp. 259268.

[23] S. Serra Capizzano 2003 *A note on anti-reflective boundary conditions and fast deblurring models*, SIAM J. Sci. Comput. **25-3** pp. 1307–1325.

[24] R. Vio, J. Bardsley, M. Donatelli, and W. Wamsteker 2005 *Dealing with edge effects in least-squares image deconvolution problems*, Astron. Astrophys. **442** pp. 397–403.